

# First observation of a rotational band in the odd-Z transfermium

## nucleus $^{251}_{101}\text{Md}$

A. Chatillon,<sup>1,\*</sup> Ch. Theisen,<sup>1</sup> E. Bouchez,<sup>1</sup> P.A. Butler,<sup>2</sup> E. Clément,<sup>1</sup>  
O. Dorvaux,<sup>3</sup> S. Eeckhautd,<sup>4</sup> B.J.P. Gall,<sup>3</sup> A. Görgen,<sup>1</sup> T. Grahn,<sup>4</sup> P.T. Greenlees,<sup>4</sup>  
R.-D. Herzberg,<sup>2</sup> F. Heßberger,<sup>5</sup> A. Hürstel,<sup>1</sup> G.D. Jones,<sup>2</sup> P. Jones,<sup>4</sup> R. Julin,<sup>4</sup>  
S. Juutinen,<sup>4</sup> H. Kettunen,<sup>4</sup> F. Khalfallah,<sup>3</sup> W. Korten,<sup>1</sup> Y. Le Coz,<sup>1,†</sup> M. Leino,<sup>4</sup>  
A.-P. Leppänen,<sup>4</sup> P. Nieminen,<sup>4,‡</sup> J. Pakarinen,<sup>4,§</sup> J. Perkowski,<sup>4</sup> P. Rahkila,<sup>4</sup>  
M. Rousseau,<sup>3</sup> C. Scholey,<sup>4</sup> J. Uusitalo,<sup>4</sup> J.N. Wilson,<sup>1,¶</sup> P. Bonche,<sup>6</sup> and P.-H. Heenen<sup>7</sup>

<sup>1</sup> *CEA-SACLAY DSM/DAPNIA/SPhN F-91191 Gif-sur-Yvette Cedex, France*

<sup>2</sup> *Oliver Lodge Laboratory, University of Liverpool, L697ZE, UK*

<sup>3</sup> *Institut de Recherches Subatomiques, F-67037 Strasbourg, France*

<sup>4</sup> *Department of Physics, University of Jyväskylä, Fin-40500, Finland*

<sup>5</sup> *GSI KP2/SHIP, D-64291 Darmstadt, Germany*

<sup>6</sup> *CEA-SACLAY DSM/DAPNIA/SPhT F-91191 Gif-sur-Yvette Cedex, France*

<sup>7</sup> *Service de Physique Nucléaire Théorique,  
Université libre de Bruxelles, B-1050 Bruxelles, Belgium*

(Dated: June 1, 2006)

### Abstract

A rotational band has been unambiguously observed in an odd-proton transfermium nucleus for the first time. An in-beam  $\gamma$ -ray spectroscopic study of  $^{251}_{101}\text{Md}$  has been performed using the  $\gamma$ -ray array JUROGAM combined with the gas-filled separator RITU and the focal plane device GREAT. The experimental results, compared to Hartree-Fock-Bogolyubov calculations, lead to the interpretation that the rotational band is built on the  $[521]1/2^-$  Nilsson state.

PACS numbers: 27.90.+b, 21.10.Re, 23.20.Lv, 25.70.Jj

The question of the heaviest chemical element that can either be found in nature or produced by man has been a fundamental one in the natural sciences, ever since D.I. Mendeleev first ordered the elements into a periodic system in 1869. The stability of atomic nuclei is governed by the shell structure of the protons and neutrons that form the nucleus. Nuclei with closed proton and neutron shells (“magic nuclei”) have enhanced stability, analogue to that of noble gases having filled electron shells, and are spherical. The heaviest known magic nucleus is  $^{208}\text{Pb}$  with 82 protons and 126 neutrons. Nuclei between closed shells can gain additional binding by taking on a non-spherical shape, due to new shell gaps that open up at finite deformation. Coulomb repulsion increases rapidly with the atomic number of the nucleus, and nuclei beyond  $Z=104$  are only bound due to such shell effects. The quest to find the next proton- and neutron- shell closures and, therefore, an island of enhanced stability at the very top of the nuclear chart, has been one of the driving forces in nuclear structure physics for many years. Theoretical prediction of the properties of super-heavy nuclei remains difficult: experimental information is scarce, due to the extremely small production cross section around 1 pb corresponding to the production rate of a few atoms per month, and the models rely on parameters adjusted for nuclei near to stability and whose reliability for exotic nuclei needs to be assessed. Slight differences of the effective interactions used in mean-field models describing super-heavy elements lead to significant deviations in the prediction of the next magic numbers. Woods-Saxon calculation predicts  $Z=114$  as the next proton spherical magic number [1], whereas  $Z=120$  and  $Z=126$  are the candidates for the relativistic mean-field [2] and Hartree-Fock-Bogolyubov (HFB) calculations [3], respectively.

One approach to improve the experimental basis on which models for super heavy elements rely, is to study in detail the collective and single-particle excitations in lighter nuclei around the deformed region at  $Z=102$ ,  $N=152$ . These transfermium nuclei (with  $Z>100$ ) are far easier to access experimentally compared to super-heavy elements. Their ground state is deformed and the low-energy spectrum of odd-mass nuclei involves orbitals that originate from above the next predicted spherical shell closure.

The nuclei in this region are the heaviest ones for which excited states can be studied using in-beam spectroscopy. Early experiments revealed the  $\alpha$ -decay fine structure of several transfermium nuclei. Only recently, with advances in experimental techniques such as recoil-tagging (RT) and more efficient detectors, have detailed spectroscopic studies in this region become possible [4]. New experimental efforts were triggered by the observation of the

rotational ground-state band of  $^{254}\text{No}$  by  $\gamma$  and electron in-beam spectroscopy [5–7]. Further rotational bands were observed in neighboring even-even nuclei [8, 9], and it was shown that these nuclei are strongly deformed ( $\beta_2 \sim 0.27$ ) and stable against fission for spins at least as high as  $20\hbar$ .

Detailed information concerning the single-particle structure and the relative position of the orbitals in the transfermium nuclei can come from the spectroscopy of odd-mass nuclei. The first evidence for a rotational band in a transfermium nucleus with odd neutron number was found in  $^{253}_{102}\text{No}$  using conversion-electron [10] and  $\gamma$ -ray spectroscopy [11].

In order to learn about the structure and position of the proton orbitals in this region, an in-beam  $\gamma$ -ray study of rotational excited states in  $^{251}_{101}\text{Md}$  was carried out at the Accelerator Laboratory of the University of Jyväskylä. A  $^{48}\text{Ca}^{10+}$  beam of intensity 7-9 pnA bombarded a  $^{205}\text{Tl}$  target of thickness  $400 \mu\text{g}/\text{cm}^2$  for approximately 220 hours.

Prompt  $\gamma$  rays were detected using the JUROGAM array consisting of 43 Compton-suppressed germanium detectors. The fusion-evaporation residues were separated from fission fragments, beam- or target-like reaction products, and the primary beam by the gas-filled separator RITU [12]. The transmitted ions are detected at the focal plane using the GREAT focal plane spectrometer [13]. The characteristic energy loss of the ions reaching the focal plane is measured with a multi-wire proportional counter (MWPC). The ions are subsequently implanted into an array of two double-sided silicon strip detectors (DSSD), each with dimensions  $60 \text{ mm} \times 40 \text{ mm} \times 300 \mu\text{m}$ . The various components of the detection system run independently in a triggerless mode (Total Data Readout [14]) and are synchronized and time-stamped with a resolution of 10 ns by a common clock. Each recoil that is identified by its energy loss and time-of-flight between the MWPC and the DSSD can be correlated with the prompt  $\gamma$  radiation measured at the target position. The RT technique allows the  $\gamma$  rays emitted by fusion-evaporation residues to be distinguished from those due to the dominant fission background.

Initially, the excitation function of the reaction was measured by changing the beam energy in steps of 3 MeV and counting the characteristic  $\alpha$ -decays of  $^{251}\text{Md}$ . The result is shown in Fig. 1 and compared to the results obtained using the HIVAP code [15], based on statistical model transition probabilities. The highest cross-section for the 2n channel leading to  $^{251}\text{Md}$  was found at a center-of-target energy of  $214 \pm 2$  MeV. Assuming a transmission of RITU of 40 % and a branching ratio of  $9.5 \pm 1.0$  % for the  $\alpha$ -decay of  $^{251}\text{Md}$  [16], the measured

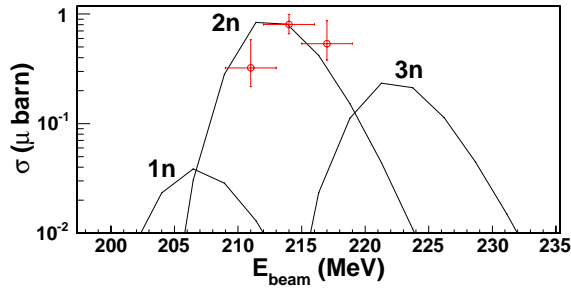


FIG. 1: Comparison between the HIVAP predictions (solid lines) and the measured cross section (points) as a function of the beam energy at the centre of the target.

rate corresponds to a production cross-section of  $\sigma=800_{-145}^{+190}$  nb. Since the cross-sections for other evaporation channels are around an order of magnitude smaller, the detection of recoils is sufficient for the identification of  $^{251}\text{Md}$  and additional selection with the characteristic  $\alpha$  decay is not required.

Gamma rays selected by the RT method are presented in the spectrum of Fig. 2b). The spectrum shows intense Md  $K_\alpha$  and  $K_\beta$  X-rays, indicating that a large fraction of the transitions proceeds via internal conversion. It is not possible to detect such converted transitions using  $\gamma$ -ray spectroscopic techniques. At least one sequence of  $\gamma$ -rays showing the characteristic regular pattern expected of a rotational band is observed. Analysis of  $\gamma - \gamma$  coincidences confirms that the candidate transitions are in mutual coincidence. Fig. 2a) shows the spectrum of  $\gamma$  rays observed in coincidence with any of the transitions marked by dashed lines. The sum of coincidence spectra reveals two transitions at higher energies, so that a total of 8 transitions are observed in the rotational sequence.

The level of statistics is not sufficient to measure the angular distribution and thus the multipolarity of the transitions. An assignment of M1 character, however, seems unlikely due to the very large internal conversion coefficients for such transitions. Assuming a  $\Delta I=2\hbar$  multipolarity, the dynamic moment of inertia  $\mathcal{J}^{(2)} = 2\Delta I/(E_\gamma(I) - E_\gamma(I - 2))$  can be extracted from the transition energies. A plot of the dynamic moment of inertia as a function of rotational frequency is shown in Fig. 3, and compared to that for neighboring even-even nuclei. The similarity of the dynamic moments of inertia supports the  $\Delta I=2\hbar$  assumption assigned to the transitions. Inspection of the  $\gamma$ -ray spectrum shown in Fig. 2 shows that only one signature of the rotational band is observed without its partner. Attempts to assign spin values to the transitions using a Harris parametrization for the moment of inertia [17, 18]

gave results extremely sensitive to the number of transitions input and were not therefore conclusive.

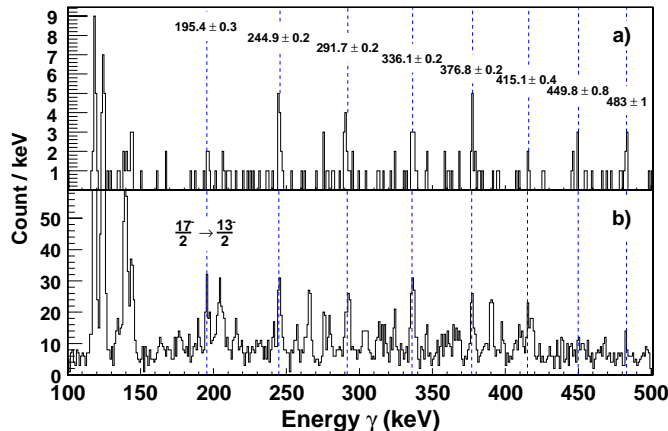


FIG. 2: Rotational band of  $^{251}\text{Md}$  obtained by RT (b) and confirmed by  $\gamma$ - $\gamma$  coincidences (a).

In recent experiments combining  $\alpha$ ,  $\gamma$  and conversion-electron spectroscopy to study the  $\alpha$  decay of  $^{255}\text{Lr}$ , the ground-state of  $^{251}\text{Md}$  has been assigned to have spin and parity  $7/2^-$ , and an excited state with spin and parity  $1/2^-$  has been observed at an excitation energy of 55 keV [16, 19]. Theoretical investigations using a Woods-Saxon potential [1] HFB calculations with a Skyrme interaction [20] predict a  $[521]1/2^-$  ground state with low-lying  $[633]7/2^+$  and  $[514]7/2^-$  excited states. HFB calculations with the Gogny interaction predict almost degenerate  $[521]1/2^-$  or  $[633]7/2^+$  orbitals at the ground state with a  $[514]7/2^-$  first excited state [21]. The  $1/2^-$ ,  $7/2^-$  and  $7/2^+$  states are therefore the three candidates for the band head of the collective structure shown in Fig. 2.

A single rotational band observed without its signature partner is usually characteristic of a  $K=1/2$  band,  $K$  being the projection of the angular momentum  $I$  on the symmetry axis. In the strong coupling limit of the particle-rotor model, bands based on a  $K=1/2$  orbital form a special case which requires the introduction of a decoupling parameter  $a$ . The non-yrast sequence  $(3/2+2n)$  sequence is shifted to higher energies compared to the yrast  $(1/2+2n)$  sequence for positive  $a$  values. The  $[521]1/2^-$  orbital is the only  $K=1/2$  candidate at low energy, and a rotational band based on the same orbital has also been observed at low spins in the lighter  $^{247}\text{Bk}$  [22] and  $^{251}\text{Es}$  [22, 23] isotopes. Decoupling parameters of 0.9 and 1, respectively, have been deduced for these two nuclei. In the case of  $a \sim 1$ , the non-yrast sequence is almost degenerate with the yrast sequence as shown in Fig. 4. The

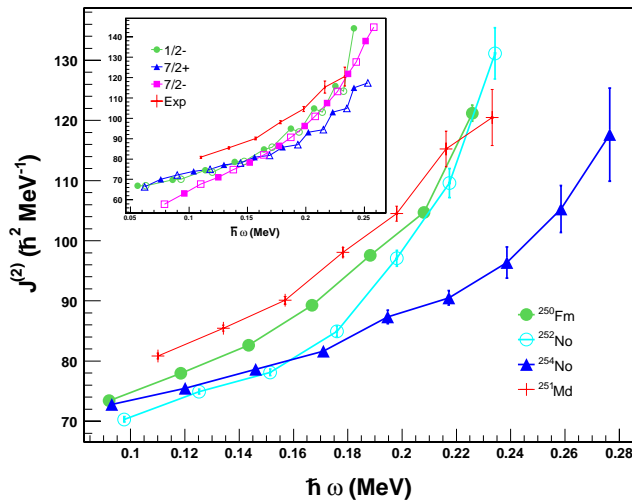


FIG. 3: Dynamical moment of inertia of the observed rotational band compared to the experimental results obtained in neighbouring even-even nuclei. Comparison with the theoretical dynamical moment of inertia is shown in the inset, where empty (filled) symbols correspond to negative (positive) signature.

signature  $\alpha = -1/2$  band feeds the  $\alpha = +1/2$  partner by M1 transitions, whereas the M1 transitions from the positive signature band are forbidden. This leads to de-excitation of the  $\alpha = +1/2$  band mainly by E2 transitions and a depopulation of the  $\alpha = -1/2$  band mostly by M1 transitions, which corresponds to our experimental observation of a single rotational sequence.

To lend weight on the  $[521]1/2^-$  assignment, new HFB calculations using the same formalism as described in Ref. [20] have been performed. The collective properties of the rotational band based on the low-lying  $1/2^-$ ,  $7/2^-$  and  $7/2^+$  states been determined. Theoretical values of the dynamic moment of inertia,  $\mathcal{J}^{(2)}$ , have been calculated for all three configurations and for both signatures (cf. Fig. 3). The  $\mathcal{J}^{(2)}$  values for all three configurations are very similar and reproduce the experimental values well, except that they underestimate the  $\mathcal{J}^{(2)}$  by  $\sim 10\hbar^2\text{MeV}^{-1}$ . As pointed out in [24], better agreement can be obtained by using quenched pairing, but there is no strong justification to adopt a new parametrization only on this basis. Comparison between the theoretical and the experimental  $\mathcal{J}^{(2)}$  is not sufficient to identify the rotational band and to understand why only one signature partner band is observed.

Therefore, the transition rates  $T(\text{M1})$  and  $T(\text{E2})$  have been extracted from the theoretical

calculations in order to determine which of the three candidates has a de-excitation scenario leading to the observation of a single signature. In odd-mass nuclei, the electromagnetic properties of rotational bands depend on the band-head configuration. To determine the transition rates, the reduced transition probabilities B(M1) and B(E2) and the intra- and inter- band transition energies have been calculated. The B(E2) can be obtained with the well-known rotational model formula [25]:

$$B(E2) = \frac{5}{16\pi} Q_0^2 \langle IK20|(I-2)K\rangle^2, \quad (1)$$

where  $Q_0$  represents the electric quadrupole moment. Rather similar  $Q_0$  values of 1320-1340 fm<sup>2</sup> are obtained for the three candidates. The B(M1) values depend not only on the band head configuration, but also on the magnetic moment  $\mu$  induced by the unpaired nucleon. For a nucleus rotating around the x axis, the B(M1) is defined as [26]:

$$B(M1) = \frac{1}{2} |\langle +|iM_1(y) + M_1(z)|-\rangle|^2, \quad (2)$$

where  $|+\rangle$  and  $|-\rangle$  are the two signature partner states linked by the M1 transition, and  $M_1(\nu)$  is the projection of the magnetic moment operator on the  $\nu$  axis. This quantity depends on orbital  $g$ -factor and the spin and angular momentum operators [26].

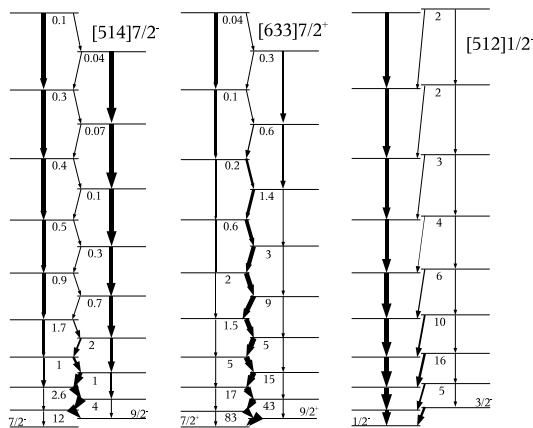


FIG. 4: Schematic decay pattern for the three configuration candidates. The number labeling the state corresponds to the total T(M1)/T(E2) transition rates.

The results show that E2 transitions are favored over M1 transitions for a band built on the  $[514]7/2^-$  configuration, whereas the opposite is true for the  $[633]7/2^+$  configuration (cf. Fig. 4). In the first case, one would expect to observe two E2 cascades of equal intensity for

both signatures, whereas in the second case no band would be observable at all due to the large conversion coefficients for the dominating M1 transitions. Our calculations shows that the  $[512]1/2^-$  configuration has a decoupling parameter  $a \sim 1$ , and only the decay pattern for the band built on this configuration is consistent with the experimental data.

Based on the transition energies calculated from the particle-rotor model, a spin assignment of  $17/2^- \rightarrow 13/2^-$  is determined for the lowest observed transition at 195.4 keV. This result is fully consistent with HFB calculations. Using the decoupling parameter and the moment of inertia, the experimental transition energies can be extrapolated to the  $1/2^-$  band head, resulting in transitions with energies of 40, 93 and 147 keV. Such transitions cannot be observed due to the large conversion coefficients and the rapid decrease of detection efficiency for  $\gamma$  rays below an energy of 200 keV.

The spectrum shown in Fig. 2b) shows evidence for several other transitions, however, no coincidence relation could be established. These transitions could correspond to the decay of the two signature-partner bands built on the  $[514]7/2^-$  orbital.

In summary, we have observed the first case of a rotational band in an odd- $Z$  transfermium nucleus. The band is observed up to spin  $45/2^-$  and has a similar moment of inertia to the neighboring even-even nuclei. The band is interpreted as being built on the  $[521]1/2^-$  configuration. This orbital originates from the spherical  $2f_{5/2}$  shell, closing the predicted  $Z=114$  spherical gap. Further investigation of other odd- $Z$  nuclei in this region is needed to study the evolution of the  $[521]1/2^-$  orbital, and the results presented here are only a first step to test the relative position of this orbital and the existence of the predicted spherical shell gap at  $Z=114$ . No spectroscopic data are presently available to test the hypotheses of shell gaps at  $Z=120$  and  $Z=126$ . The spectroscopy of highly excited states in transfermium nuclei seems the most viable approach to answer these questions in the near future.

This work has been supported by the European Union Fifth Framework Program ‘‘Improving Human Potential - Access to Research Infrastructure’’ (Contract No. HPRI-CT-1999-00044) and by the Academy of Finland under the Finnish Centre of excellence Program 2000-2005 (Project No. 44875). A. Chatillon and J. Perkowski acknowledge the receipt of funding under the Marie Curie training site programme of the EU (Contract No. HPMT-CT-2001-00250). The use of detectors in JUROGAM from the UK/France (EPSRC/IN2P3) Loan Pool and the GAMMAPOOL network is gratefully acknowledged.



---

\* Present address: GSI KP2/LAND, D-64291 Darmstadt, Germany; Electronic address: a.  
chatillon@gsi.de

† Present address: CEA Cadarache, F-13108 St Paul Lez Durance Cedex, France

‡ Present address: Department of Nuclear physics, ANU, Canberra, ACT 0200, Australia

§ Present address: Oliver Lodge Laboratory, University of Liverpool, L697ZE, UK

¶ Present address : Institut de Physique Nucléaire, IN<sub>2</sub>P<sub>3</sub>-CNRS, F-91406 Orsay, France

- [1] S. Ćwiok *et al.*, Nucl. Phys. **A573**, 356 (1994).
- [2] K. Rutz *et al.*, Phys. Rev. C **56**, 238 (1997).
- [3] M. Bender *et al.*, Phys. Rev. C **60**, 034304 (1999).
- [4] M. Leino, F.P. Hessberger, Ann. Rev. Nucl. Part. Sci. **54**, 175 (2004).
- [5] P. Reiter *et al.*, Phys. Rev. Lett. **82**, 509 (1999).
- [6] M. Leino *et al.*, Eur. Phys. J. A **6**, 63 (1999).
- [7] P.A. Butler *et al.*, Phys. Rev. Lett. **89**, 202501 (2002).
- [8] R.-D. Herzberg *et al.*, Phys. Rev. C **65**, 014303 (2001).
- [9] J. E. Bastin *et al.*, Phys. Rev. C **73**, 024308 (2006).
- [10] R.-D. Herzberg *et al.*, Eur. Phys. J. A **15**, 205 (2002).
- [11] P. Reiter *et al.*, Phys. Rev. Lett. **95**, 032501 (2005).
- [12] M. Leino *et al.*, Nucl. Instr. Meth **B99**, 653 (1995).
- [13] R. D. Page *et al.*, Nucl. Instr. Meth **B204**, 634 (2003).
- [14] I. H. Lazarus *et al.*, IEEE Trans. Nucl. Sci. **48**, p567 (2001).
- [15] W. Reisdorf, Z. Phys. **A 300**, 227 (1981).
- [16] A. Chatillon *et al.*, to be published.
- [17] J. A. Becker *et al.*, Phys. Rev. C **41**, R9 (1990).
- [18] J. E. Draper *et al.*, Phys. Rev. C **42**, R1791 (1990).
- [19] F. Heßberger *et al.*, Eur. Phys. J. A **26**, 233 (2005).
- [20] M. Bender *et al.*, Nucl. Phys. **A723**, 354 (2003).
- [21] H. Goutte, private communication.
- [22] I. Ahmad *et al.*, Phys. Rev. Lett. **39**, 12 (1977).
- [23] I. Ahmad *et al.*, Phys. Rev. C **17**, 2163 (1978).

- [24] T. Duguet, P. Bonche, P.-H. Heenen, Nucl. Phys. **A679**, 427 (2001).
- [25] A. Bohr, B. Mottelson, *Nuclear Structure, Volume 2*, W. A. Benjamin, INC., 1969.
- [26] I. Hamamoto and H. Sagawa, Nucl. Phys. **A327**, 99 (1979).